Article Summary Line: We identified respiratory, nosocomial and bacterial pathogens as prevalent microorganisms in 21 Brazilian COVID-19 patients admitted to Intensive Care Units. Pathogen virulence factors and immune response evasion metabolic pathways are correlated to COVID-19 severity.

Running Title: Bacterial pathogens in Brazilian COVID-19 severity

Keywords: COVID-19, Bacteria, Respiratory Tract Infections, Bioinformatics

Title

Prevalence of bacterial pathogens and potential role in COVID-19 severity in patients admitted to intensive care units in Brazil

Authors:

Fabíola Marques de Carvalho[1], Leandro Nascimento Lemos[1], Luciane Prioli Ciapina[1], Rennan Garcias Moreira[2] , Alexandra Gerber[1], Ana Paula C Guimarães[1], Tatiani Fereguetti[3], Virgínia Antunes de Andrade Zambelli[3], Renata Avila[3], Tailah Bernardo de Almeida[4] , Jheimson da Silva Lima[5], Shana Priscila Coutinho Barroso[6], Mauro Martins Teixeira[2], Renan Pedra Souza[2], Cynthia Chester Cardoso[7], Renato Santana Aguiar[2], Ana Tereza Ribeiro de Vasconcelos[1]#

Affiliations:

[1] Laboratório Nacional de Computação Científica, Petrópolis, Brazil (F.M. Carvalho, L.N. Lemos, L.P. Ciapina, A. Gerber, A.P.C. Guimarães, A.T.R. Vasconcelos)

[2] Instituto de Ciências Biológicas, Universidade Federal de Minas Gerais, Belo Horizonte, Brazil (R. Moreira, M. M. Teixeira, R. P. Souza, R. S. Aguiar)

[3] Hospital Eduardo de Menezes, Belo Horizonte, Brazil (T. Fereguetti, V. A. A. Zambelli, R. Avila)

[4] Instituto de Estudos do Mar Almirante Paulo Moreira, Marinha do Brasil, Rio de Janeiro, Brazil (T. B.Almeida)

[5] Unidade de tratamento de queimados, Hospital Naval Marcílio Dias, Rio de Janeiro, Brazil (J. S. Lima)

[6] Instituto de Pesquisas Biomédicas, Hospital Naval Marcílio Dias, Rio de Janeiro, Brazil (S. P. C. Barroso)

[7] Instituto de Biologia, Universidade Federal do Rio de Janeiro, Rio de Janeiro, Brazil (C. C, Cardoso)

corresponding author

Abstract

Secondary bacterial and fungal infections are associated with respiratory viral infections and invasive mechanical ventilation. In Coronavirus disease 2019 (COVID-19), lung injury by SARS-CoV-2 and impaired immune response can provide a favorable environment for microorganism growth and colonization in hospitalized individuals. Recent studies suggest that secondary bacterial pneumonia is a risk factor associated with COVID-19. In Brazil, knowledge about microbiota present in COVID-19 patients is incipient. This work describes the microbiota of 21 COVID-19 patients admitted to intensive care units from two Brazilian centers. We identified respiratory, nosocomial and bacterial pathogens as prevalent microorganisms. Other bacterial opportunistic and commensal species are also represented. Virulence factors of these pathogenic species, metabolic

pathways used to evade and modulate immunological processes and the interconnection between bacterial presence and virulence in COVID-19 progression are discussed.

Introduction

Severe COVID-19 cases are characterized by systemic hyperinflammation and immune dysfunction, which may lead to lung damage. Infection begins with the internalization of the viral complex through the interaction between SARS-CoV-2 spike protein and the angiotensin-converting enzyme 2 (ACE2) in the host cell. ACE2 expression reduces after SARS-CoV-2-infection, resulting in an increase in angiotensin II which lead to pathophysiological effects that include vasoconstriction, increased inflammation and fibrosis (*1*). Lung edema, endothelial and epithelial injuries are accompanied by an influx of neutrophils into the interstitium and bronchoalveolar space, resulting in impairment of arterial oxygenation (*2*). Infection of alveolar macrophages by SARS-CoV and neutrophil infiltration are important triggers of the cytokine storm, which is extensively associated with COVID-19 severity and mortality (*3*).

In the critical stage of COVID-19, cytokine storm is continuous, contributing to vascular congestion, complement cascade activation and over disseminated intravascular coagulation (*4*). Hypoxia is aggravated and invasive mechanical ventilation may be required for life maintenance. Under these conditions, variation in oxygen tension, alveolar ventilation, deposition of inhaled particles, blood flow and concentration of inflammatory cells are factors that directly affect lung microbial growth conditions (*5, 6*). In addition, irregular innate immune response in acute lung injury, mainly during the process of neutrophil recruitment, may favor bacterial infections, which are also regulated by virulence factors (*7*).

In Influenza and Severe Acute Respiratory Syndrome (SARS), secondary bacterial infection has been reported during intensive care unit admission and during use of invasive mechanical

ventilation. Data in literature pointed out that occurrence of co-infection or secondary bacterial pneumonia was observed in 11% to 35% of individuals with laboratory confirmed influenza (*8*), and that *Streptococcus pneumoniae* and *Staphylococcus aureus* were present in 35% and 28% of patients, respectively. In Canada, *Chlamydophila pneumoniae* or *Mycoplasma pneumoniae* were abundant in up to 30% of SARS patients (*9*). Bacterial infection was also identified in COVID-19 cases (*10* - *12*). Studies conducted in China, the USA, Spain and Thailand, showed that secondary bacterial infection was present in 14% of patients, with occurrence of *Streptococcus pneumoniae*, *Klebsiella pneumoniae* and *Haemophilus influenzae* within 1–4 days of COVID-19 disease onset (*13,14*). According to Rawson et al. (2020)(*15*), the extensive use of broad-spectrum antibiotics can predispose COVID-19 patients to acquisition of bacterial infections and increase multidrug-resistance.

Colonizing species in patients infected with SARS-CoV-2, prevalence of bacterial infection and mechanism of co- or secondary-infection remain poorly understood. In Brazil, an investigation of bacterial microbiota in SARS-CoV-2 was conducted in only one patient and concise results showed the predominance of *Lautropia*, *Prevotella* and *Haemophilus* genera (*16*). In-depth work was not performed.

This study aims to determine the microbiota of 21 COVID-19 patients admitted to intensive care units from two Brazilian centers, focusing on prevalence of bacterial pathogens, and to correlate the microbiota with the immunological disorder characteristic of Coronavirus disease 2019.

Material and Methods

Study cohort and data collection. Twenty-one COVID-19 patients admitted to Intensive Care Units (ICU) from Hospital Naval Marcílio Dias (Rio de Janeiro) and Hospital Eduardo de Menezes

(Belo Horizonte) were included in this study. Both hospitals are located in cities in the Southeast region of Brazil. All patients had positive RT-PCR tests for SARS-CoV-2 (Table 1). Samples identification (IDs) were modified to preserve the patient's integrity. The study cohort included 12 males and 9 females and no age restrictions were applied (ranging from 37 to 89 years of age).The present study was approved by the Ethics Commission from Hospital Naval Marcílio Dias and Hospital Eduardo de Menezes (protocol number 32382820.3.0000.5256 and 31462820.3.0000.5149). Clinical and demographic characteristics of the 21 patients were obtained from medical records and summarized in Table1.

DNA extraction and sequencing. DNA was extracted using standard manufacturer's protocols for the Qiagen QIAamp DNA Microbiome kit (Qiagen, Germany). Metagenomic libraries were constructed using the Nextera DNA Flex Library Preparation Kit (Illumina, USA). Sequencing was performed in a NextSeq 500 System with a NextSeq 500/550 High Output Kit v2.5 (300 Cycles) (Illumina, USA).

Bioinformatics analysis.

Sequencing files were submitted to MG-RAST (version 4.0.3) (*17)* for taxonomical and functional inferences. Sequences were trimmed using default parameters and human sequences removed by screening against *Homo sapiens*. Species were identified from MG-RAST using RefSeq and functional abundances were obtained using SEED subsystem database. For both analyses, the Best Hit Classification criteria and alignment cutoff applied included an e-value > 10^{-5}, a minimum identity of 60%, and a minimum alignment of 15. Low abundance species (≤ 50 absolute counts of the sum of all samples) were removed to avoid false-positives and minimize the error of taxonomical predictions (*18*). The number of species was resampled so that all samples had the

same library size. Prevalent species were detected using the microbiome R package (*19*), considering only those that occurred in 75% of all patients. Phyloseq R package was used to estimate the Shannon diversity index (*20*).

Results and Discussion

The study included only adult patients, the majority of whom were above 65 years of age (42.8%). Males represent 57% of the patients sampled. The period between symptom onset and sample collection varied from 4 to 34 days. All individuals were admitted to intensive care units and invasive ventilatory support was necessary in 95.2% of the cases. No previous pulmonary impairment was reported, except for one individual. Most patients had at least one of the main comorbidities associated with disease severity. Diabetes represented 50% of the cases studied, followed by obesity and hypertension (33% in both) and cardiovascular disease (23.8%) (Table 1). Tracheal lavage samples with SARS-CoV-2 infectivity had higher abundances of bacterial respiratory and nosocomial species (Table 2). To check the relationship between microbial diversity and the proportion of microbial pathogens, we estimated diversity using the Shannon index and calculated the relative abundance of pathogens (Figure 1). The proportion of microbial pathogens was based on the relative abundance of individual pathogens divided by the total number of species in the microbiome. First, we observed a negative correlation (-0.9733005; $p \leq 0.05$) between these two parameters, indicating that the prevalence of pathogens in all samples is inverse to diversity, causing a decrease in species richness. A high proportion of pathogens can be explained by the potential imbalance between microbial immigration and elimination, and regional growth conditions, as proposed by Dickson and collaborators (2015)(*21*).

Dickson and collaborators (2014, 2015) (*6, 21*) report that, while in healthy lungs the immigration and elimination processes are more determinant for microbial composition, in

advanced lung diseases, pulmonary pathogenesis is a consequence of respiratory dysbiosis. Hyperventilation accelerates the influx of air-borne microbes and microbial elimination is reduced by bronchoconstriction and impaired mucociliary clearance. This condition provides a nutrient-rich growth medium and decreased oxygen concentration, influencing bacterial reproduction. In addition, these authors propose that the response to inflammation and endothelial and epithelial injury increases vascular permeability, promoting the escape of nutrient-rich fluid into the alveolar compartment, restoring the nutrient supply and selectively favoring the growth of specific lung pathogens. Our results suggest that COVID-19 reduces microbial diversity and increases the proportion of pathogens, similar to other acute and chronic lung diseases (O'Dwyer et al., 2015) (*22*).

Almost 75% of the microbiota present in patients was composed of bacteria whose diversity was inferred from the fifty most prevalent species (Figure 2 and Table 2). Most respiratory pathogens were composed of *Acinetobacter baumannii* (corresponding to 16.5% of all bacterial species), *Streptococcus pneumoniae* (8.8%), *Pseudomonas aeruginosa* (3.6%) and *Staphylococcus aureus* (3.4%). Nosocomial pathogens mainly included fungi *Candida albicans* and *Candida tropicalis,* representing 11.2% and 8.1% of Eukarya domain, as well as the bacteria *Enterococcus faecalis* (1.5%) *and Escherichia coli* (0.5%). The presence of most of these pathogens is in concordance with the microbiota reported in patients from China, France and Iran (*28 - 31*).

Furthermore, the patients analyzed in our work showed a diversity of other pathogenic microorganisms, such as the uncommon *Listeria monocytogenes*, *Streptococcus* (*S. agalactiae* and *S. pyogenes*), sporulating *Bacillus* (*B. anthracis* and *B. thuringiensis*) and *Acidovorax spp.,* although less frequently (Figure 2). Curiously, the opportunistic microorganisms *Delftia acidovorans* and *Coprobacillus spp.* were found with an abundance of almost 6% and 2%, respectively. *Delftia*

acidovorans is usually not pathogenic, but catheter-related bacteremia and cases of pneumonia with lung cavity formation has been observed (*23, 24*).

As expected, an elevated occurrence of the bacterial respiratory pathogen *Streptococcus pneumoniae* was found independent of the comorbidity, while in patients without comorbidity the occurrence of respiratory and nosocomial pathogens was drastically reduced, with exception of *Candida albicans* and *Candida tropicalis* (Figure 2 and Table 2). In contrast, *Acinetobacter baumannii* was significantly increased in patients with higher SARS-CoV2 infection period (RJ2 and RJ3 samples). No significant difference or direct association was observed between pathogen abundance and comorbidity type. However, the microbiota here identified reinforce the severity of infection under weakened health conditions.

Additionally, a large diversity of the oropharynx commensal species was identified, such as *Rothia mucilaginosa*, *Parvimonas micra*, *Actinomyces odontolyticus*, and *Streptococcus anginosus* (Table 2). *R. mucilaginosa* has been associated to pneumonia in patients with chronic obstructive pulmonary disease (COPD) (*25*). Furthermore, an association of co-infection by *A. odontolyticus and P. micra* or *Streptococcus spp*. to lung abscess and acute respiratory failure was reported (*26, 27*). Although respiratory disease caused by these commensals is a rare event, their presence in individuals with compromised immune responses should not be neglected.

The bacterial pathogens identified in this study, particularly *Acinetobacter baumannii*, *Streptococcus pneumoniae*, *Pseudomonas aeruginosa* and *Staphylococcus aureus*, may promote virulence and evade the host immune response by biofilm production, induction of hemolysins, pneumolysin, phospholipases, iron acquisition factors, cytokines, adhesins, and complement system resistance, besides other virulence factors (*28 - 30*).

In pulmonary and catheter-associated infections, biofilm formation can be favored by microbial interaction in endotracheal tubes and mechanical-ventilation apparatus, resulting in a

diverse microbial complex and enhanced antimicrobial resistance (*31*,*32*). Studies demonstrated that *A. baumannii, Klebsiella pneumoniae*, and *Enterococcus faecium* are also frequently recovered from endotracheal tubes (*33*-*35*). In addition, in clinical isolates with persistent infections, *P. aeruginosa, S. aureus* and *C. albicans* are the predominant biofilm-producers and species with more biofilm formation capacity are frequently observed to be multidrug-resistant (*36*-*38*). For some of these microorganisms, the increase of biofilm, production of bacterial virulence factors and antibiotic resistance are related to enrichment of macrophage secretory products in culture and oxygen-limiting conditions (*39, 40*). In *S. aureus,* for example, biofilm is related to accumulation of activated macrophages exhibiting anti-inflammatory and pro-fibrotic properties (*41*). Moreover, it was observed that, when in biofilm, bacterial species are more resistant to the immune response, evading neutrophil mediated phagocytosis (*42*).

Hemolysin, an important virulence factor of *S. aureus*, *E. coli*, and *Enterococcus faecalis* (*43*, *44*), is a protein that causes erythrocyte lyse and disrupts the cell membrane, contributing to lung injury and pneumonia. In *Streptococcus pneumoniae*, when pulmonary surfactant is deficient, there is an expression of hemolysin, which is correlated with lung epithelial cell injury and induction of interleukin (IL)–8 (*45*).

Similar to hemolysin, pneumolysin is a pore-forming toxin, and most of its isoforms exhibit hemolytic activity. This protein is crucial for virulence and chronic bacteraemia of *Streptococcus pneumoniae*, and together with polysaccharide capsule proteins and adhesins reduce the *S. pneumoniae* entrapment in the pulmonary mucus, permitting adherence and inflammatory responses and activating complement and apoptosis (*46*).

For *Candida* species identified in this work, phospholipase and biofilm are described as the major virulence factors (*47, 48*). Phospholipases possess an important role in lung diseases,

promoting change in membrane composition, stimulating chemokines and cytokines, and altering gas exchange and as a lung surfactant (*49*).

Hemolysin, phospholipase and biofilm are some of the many pathogenicity factors in *Acinetobacter baumannii*. Successful fitness of this bacteria, however, is a consequence of a large virulence repertoire, also composed by outer membrane proteins, secretion systems, surface adhesins, glycoconjugates and iron-chelating activities, which can explain its multi-resistance to antibiotics in nosocomial infections (*28*).

Biofilm-based infections are significantly less susceptible to antimicrobial agents and their treatment is extremely difficult. According to Sanchez et al., 2013 (*37*), the investigation of biofilm forming capacity in patients with diverse infective sources revealed that *Staphylococcus aureus*, *Acinetobacter baumannii*, *Pseudomonas aeruginosa*, *Klebsiella pneumoniae*, and *Escherichia coli* are strong biofilm producers, at levels greater than or equal to *Staphylococcus epidermidis*, a positive biofilm producing strain. The greatest number of biofilm producing strains corresponded to *P. aeruginosa* and *S. aureus* species.

Interestingly, the metabolic profile obtained in our study correlated to virulence factors of the species described, particularly biofilm (Tables 3-6). Within Central Carbohydrate Metabolism (Table 3), the TCA_cycle was the predominant pathway (18%), with abundance of dihydrolipoamide dehydrogenase enzyme (Table 4). According to Lu and authors (2019) (*50*), alteration in the metabolites from the TCA cycle, amino acid metabolism, and glycerolipid pathways were observed during biofilm production. Furthermore, characterization of dihydrolipoamide dehydrogenase from *Streptococcus pneumoniae* showed that this enzyme plays an important role in pneumococcal infection, being necessary for the survival and capsular polysaccharide production of pneumococci within the host (*51*).

Besides enzymes associated with biofilm formation, we identified adhesins, permeases for antibiotic export, resistance and toxins, and superantigens belong to the Virulence, Disease and Defense functional category (Table 5). The most abundant adhesins are fibronectin/fibrinogen-binding proteins, although high numbers of sortases, related to attachment of specific proteins to the cell wall, were also found. Toxins and superantigens are composed of the streptolysin S locus, which produces the beta-haemolytic phenotype. Streptolysin S causes impaired phagocytic clearance and promotes epithelial cell cytotoxicity, enhancing the effects of M protein and streptolysin O (*52*). In the Membrane Transport category, protein secretion system Types I, V, and VI are highlighted, with abundance of exoprotein involved in heme utilization, cytolysin activator and adhesin (Table 6).

The scenario highlights the high occurrence of potentially virulent pathogens, which can contribute to severity of lung infection in Coronavirus Disease 2019 patients admitted to intensive care units. Moreover, the prevalence of respiratory pathogens observed in COVID-19 patients analyzed can be orchestrated mainly by the complex and distinct immune events in response to lung damage, as well as by the ecological model proposed by Dickson and collaborators (2014, 2015) (*26*, *25*), which indicate that several lung diseases can alter the growth of local microbiota, leading to an increase in bacterial abundance. A cellular model to explain the bacterial species described in our study correlated to processes that aggravate COVID-19 is presented (Figure 3).

Impairment in neutrophil function, macrophage depletion and excessive inflammation has been reported as an important factor in the progression of lower respiratory tract pathologies (*53*). It was demonstrated that alveolar macrophage depletion could facilitate the bacterial infection by the establishment of a niche for secondary *Streptococcus pneumoniae* infection, altering cellular innate immunity and resulting in lethal pneumonia (*54*). Additionally, neutrophilia plays an important role in bacterial pulmonary diseases, including those caused by *Streptococcus pneumoniae, Klebsiella*

pneumoniae, *Haemophilus influenzae*, and *Staphylococcus aureus* (*55*). Interestingly, Sodhi and collaborators (2019) (*56*) demonstrated that impaired neutrophil and innate immune response might be mediated by variations in the activity of angiotensin-converting enzyme 2 (ACE2). In bacterial lung infection, when pulmonary active ACE2 levels vary dynamically, neutrophil influx increases, compromising the host-defense capability and heightened inflammatory response, with subsequent elevation of infection severity and mortality

Similar to Coronavirus Disease 2019, patients with chronic obstructive pulmonary disease (COPD) show vascular permeabilization, platelet activation, thrombosis, adhesion molecule expression, leukocyte recruitment, and complement activation, which are also observed in injury-derived free heme (*57*). Su and authors (2020)(*58*) observed increased heme and heme oxygenase (HO)-1 in the blood system of severe COVID-19 patients. Moreover, an additional role of hemoglobinopathy, hypoxia and hyperferritinemia has been proposed in worsening COVID-19 infection (*59, 60*).

Increase of cell-free hemoglobin (Hb) and HO-1 expression in lung tissue and bronchoalveolar lavage fluid has been correlated to COPD and acute respiratory distress syndrome (ARDS) severity (*61*). Simon and authors (2009)(*62*) demonstrated an ACE-like activity of Hb in the conversion of angiotensin I to its active metabolites induced by ferrous- and ferryl-Hb, with a possible effect on vasoconstriction. Moreover, intratracheal administration of heme in mice led to alveolar-capillary barrier dysfunction and increased alveolar permeability, contributing to acute lung and ARDS (*63*). Curiously, heme uptake by pathogens plays an important role during bacterial infection. These microorganisms induce erythrocyte hemolysis caused by pore-forming toxins, such as hemolysin and phospholipases. Free-heme and iron acquired from erythrocyte disruption is required for invasion, growth and successful pathogen colonization in the host (*64*). In addition, Dutra and collaborators (2014)(*65*) showed that heme promotes the processing of caspase-1,

inflammasome activation and IL-1β secretion by macrophages that participate in the immune response induced by hemolysis, contributing to inflammation and pathogenesis. Strategies for interfering in inflammasome activation by bacterial pathogens have evolved (*66*), and together with SARS-Cov2, may contribute to a hyperactivated inflammatory response (*67*).

Interdependence between iron acquisition and virulence factors for bacterial pathogenesis have been demonstrated. In *Streptococcus pneumoniae*, iron is a critical factor for regulation of several enzymes. During pneumonia and bacteremia, the transcription of hemolysin, toxins, cell wall hydrolases and biofilm formation are increased in a positive Fe-dependent regulation (*68*). For *Pseudomonas aeruginosa*, high iron concentrations are correlated to stimulation of aggregation, adhesion and biofilm formation, in a positive-modulation manner (*69*). The acquisition of heme-iron bound to erythrocyte hemoglobin is the preferred source of iron during *S. aureus* infection initiation, as well as for its proliferation. In the presence of heme, regulatory systems induced exotoxins such as cytolysins, proteases, and other virulence factors, promote Staphylococcal cellular adherence to host cells and resistance to neutrophil killing. Furthermore, iron and oxygen conditions have been shown to influence the TCA cycle activity of *Staphylococcus aureus* (*70 - 72*). Free-iron uptake by ferritin and haemolytic activity is employed by *Candida albicans*. Interestingly, it has been speculated that co-habitation of *C. albicans* with both commensal and pathogenic bacteria, in a synergistic interaction, enables *C. albicans* to obtain iron more easily (*73*).

In conclusion, the presence of respiratory pathogens, nosocomial bacteria and opportunistic microorganisms during colonization of the host, secrete an extensive diversity of virulence factors. These molecules favor hemolysis, cytokine activation and inflammation. The presence of free-iron exacerbates bacterial pathogenesis in cyclic connection with the worsening of the immune response, favoring the resistance of bacterial species. These findings provide intriguing insights into SARS-CoV2-bacterial interactions contributing to COVID-19 severity.

Data availability

NGS data generated in our study is publicly available in SRA-NCBI (www.ncbi.nlm.nih.gov/sra), Bioproject accession PRJNA683652.

Acknowledgments

This work was developed under the frameworks of Corona-ômica-RJ (FAPERJ = E-26/210.179/2020) and Rede Corona-ômica BR MCTI/FINEP (FINEP = 01.20.0029.000462/20, CNPq = 404096/2020-4). A.T.R.V. is supported by Conselho Nacional de Desenvolvimento Científico e Tecnológico - CNPq (303170/2017-4) and FAPERJ (E-26/202.903/20). R.S.A. is supported by CNPQ 312688/2017-2, 439119/2018-9; FAPERJ 202.922/2018 .C.C.C is supported by FAPERJ (E-26/202.791/2019) and S.P.C.B is supported by FAPERJ (E-26/010.000168/20).

Author Bio

F.M.C is currently a postdoctoral fellow in the Laboratory of Bioinformatics (LABINFO) of the National Laboratory of Scientific Computing (LNCC). Research interests comprise metagenomic (clinical and environmental) and comparative genomics.

References

1. Bourgonje AR, Abdulle AE, Timens W, Hillebrands JL, Navis GJ, Gordijn SJ, et al. Angiotensin-converting enzyme 2 (ACE2), SARS-CoV-2 and the pathophysiology of coronavirus disease 2019 (COVID-19). J Pathol. 2020;251:228-48.
2. Abraham E. Neutrophils and acute lung injury. Crit Care Med. 2003;31:S195–9.

3. Channappanavar R, Perlman S. Pathogenic human coronavirus infections: causes and consequences of cytokine storm and immunopathology. Semin. Immunopathol. 2017;39:529–39.
4. Tang N, Li D, Wang X, Sun Z. Abnormal coagulation parameters are associated with poor prognosis in patients with novel coronavirus pneumonia. J. Thromb. Haemost. 2020;18: 844–47.
5. West JB. Regional differences in the lung. Chest. 1978;74:426-37.
6. Dickson RP, Martinez FJ, Huffnagle GB. The role of the microbiome in exacerbations of chronic lung diseases. Lancet. 2014;384:691-702.
7. Balamayooran G, Batra S, Fessler MB, Happel KI, Jeyaseelan S. Mechanisms of neutrophil accumulation in the lungs against bacteria. Am J Respir Cell Mol Biol. 2010;43:5-16.
8. Klein EY, Monteforte B, Gupta A, Jiang W, May L, Hsieh YH, et al. The frequency of influenza and bacterial coinfection: a systematic review and meta-analysis. Influenza Other Respir Viruses. 2016;10:394-403.
9. Zahariadis G, Gooley TA, Ryall P, Hutchinson C, Latchford MI, Fearon MA, et al. Risk of ruling out severe acute respiratory syndrome by ruling in another diagnosis: variable incidence of atypical bacteria coinfection based on diagnostic assays. Can Respir J. 2006;13:17-22.
10. Vaillancourt M, Jorth P. The Unrecognized Threat of Secondary Bacterial Infections with COVID-19. mBio. 2020;11:e01806-20.
11. Bengoechea JA, Bamford CG. SARS-CoV-2, bacterial co-infections, and AMR: the deadly trio in COVID-19?. EMBO Mol Med. 2020;12:e12560.
12. Manohar P, Loh B, Nachimuthu R, Hua X, Welburn SC, Leptihn S. Secondary Bacterial Infections in Patients With Viral Pneumonia. Front Med (Lausanne). 2020;7:420.

13. Zhu X, Ge Y, Wu T, Zhao K, Chen Y, Wu B, et al. Co-infection with respiratory pathogens among COVID-2019 cases. Virus Res. 2020;285:198005.
14. Langford BJ, So M, Raybardhan S, Leung V, Westwood D, MacFadden DR, et al. Bacterial co-infection and secondary infection in patients with COVID-19: a living rapid review and meta-analysis. Clin Microbiol Infect. 2020;22:30423-7.
15. Rawson TM, Moore LSP, Zhu N, Ranganathan N, Skolimowska K, Gilchrist M, et al. Bacterial and fungal co-infection in individuals with coronavirus: A rapid review to support COVID-19 antimicrobial prescribing. Clin Infect Dis. 2020;2:ciaa530.
16. Chakraborty S. Metagenome of SARS Cov2 from a patient in Brazil shows a wide range of bacterial species Lautropia, Prevotella, Haemophilus overshadowing viral reads, which does not even add up to a full genome, explaining false negatives. OSF Preprints; 2020.
17. Meyer F, Paarmann D, D'Souza M, Olson R, Glass EM, Kubal M, et al.The metagenomics RAST server – a public resource for the automatic phylogenetic and functional analysis of metagenomes. BMC Bioinformatics. 2008;9:386.
18. Ye SH, Siddle KJ, Park DJ, Sabeti PC. Benchmarking Metagenomics Tools for Taxonomic Classification. Cell. 2019;178:779-94.
19. Leo Lahti, Sudarshan Shetty et al. Tools for microbiome analysis in R.; 2017. URL: http:// microbiome.github.com/microbiome.
20. McMurdie PJ, Holmes S. phyloseq: an R package for reproducible interactive analysis and graphics of microbiome census data. PLoS One. 2013;8:e61217.
21. Dickson RP, Erb-Downward JR, Freeman CM, McCloskey L, Beck JM, Huffnagle GB, et al. Spatial Variation in the Healthy Human Lung Microbiome and the Adapted Island Model of Lung Biogeography. Ann Am Thorac Soc. 2015;12:821-30.

22. O'Dwyer DN, Dickson RP, Moore BB. The Lung Microbiome, Immunity, and the Pathogenesis of Chronic Lung Disease. J Immunol. 2016;196:4839-47.
23. Yildiz H, Sünnetçioğlu A, Ekin S, Baran Aİ, Özgökçe M, Aşker S, et al. *Delftia acidovorans* pneumonia with lung cavities formation. Colomb Med (Cali). 2019;50:215-21.
24. Patel D, Iqbal AM, Mubarik A, NiraliVassa, RaniaGodil, Mohamad Saad, et al. *Delftia acidovorans*: A rare cause of septic pulmonary embolism from catheter-related infection: Case report and literature review. Respir Med Case Rep. 2019;27:100835.
25. Maraki S, Papadakis IS. *Rothia mucilaginosa* pneumonia: a literature review. Infect Dis (Lond). 2015;47:125-9.
26. Yun SS, Cho HS, Heo M, Jeong JH, Lee HR, Ju S, et al. Lung abscess by *Actinomyces odontolyticus* and *Parvimonas micra* co-infection presenting as acute respiratory failure: A case report. Medicine (Baltimore). 2019;98(35):e16911.
27. Takiguchi Y, Terano T, Hirai A. Lung abscess caused by *Actinomyces odontolyticus*. Intern Med. 2003;42:723-5.
28. Harding C, Hennon S, Feldman M. Uncovering the mechanisms of *Acinetobacter baumannii* virulence. Nat Rev Microbiol. 2018; 16:91–102.
29. Kadioglu A, Weiser J, Paton J, Andrew PW. The role of *Streptococcus pneumoniae* virulence factors in host respiratory colonization and disease. Nat Rev Microbiol. 2018;6:288–301.
30. Bien J, Sokolova O, Bozko P. Characterization of Virulence Factors of *Staphylococcus aureus*: Novel Function of Known Virulence Factors That Are Implicated in Activation of Airway Epithelial Proinflammatory Response. J Pathog. 2011;2011:601905.

31. Adair CG, Gorman SP, Feron BM, Byers LM, Jones DS, Goldsmith CE, et al. Implications of endotracheal tube biofilm for ventilator-associated pneumonia. Intensive Care Med. 1999;25:1072-6.
32. Wolcott R, Costerton JW, Raoult D, Cutler SJ. The polymicrobial nature of biofilm infection. Clin Microbiol Infect. 2013;19:107-12.
33. Cardeñosa Cendrero JA, Solé-Violán J, Bordes Benítez A, Noguera Catalán J, Arroyo Fernández J, Saavedra Santana P, et al. Role of different routes of tracheal colonization in the development of pneumonia in patients receiving mechanical ventilation. Chest. 1999;116:462-70.
34. Gil-Perotin S, Ramirez P, Marti V, Sahuquillo JM, Gonzalez E, Calleja I, et al. Implications of endotracheal tube biofilm in ventilator-associated pneumonia response: a state of concept. Crit Care. 2012;16:R93.
35. Vandecandelaere I, Matthijs N, Van Nieuwerburgh F, Deforce D, Vosters P, De Bus L, et al. Assessment of microbial diversity in biofilms recovered from endotracheal tubes using culture dependent and independent approaches. PLoS One. 2012;7:e38401.
36. Boisvert AA, Cheng MP, Sheppard DC, Nguyen D. Microbial Biofilms in Pulmonary and Critical Care Diseases. Ann Am Thorac Soc. 2016;13:1615-23.
37. Sanchez CJ Jr, Mende K, Beckius ML, Akers KS, Romano DR, Wenke JC, et al. Biofilm formation by clinical isolates and the implications in chronic infections. BMC Infect Dis. 2013;13:47.
38. Mittal R, Sharma S, Chhibber S, Harjai K. Effect of macrophage secretory products on elaboration of virulence factors by planktonic and biofilm cells of *Pseudomonas aeruginosa*. Comp Immunol Microbiol Infect Dis. 2006;29:12-26.

39. Borriello G, Werner E, Roe F, Kim AM, Ehrlich GD, Stewart PS. Oxygen limitation contributes to antibiotic tolerance of *Pseudomonas aeruginosa* in biofilms. Antimicrob Agents Chemother. 2004;48:2659-64.
40. Hanke ML, Kielian T. Deciphering mechanisms of staphylococcal biofilm evasion of host immunity. Front Cell Infect Microbiol. 2012;2:62.
41. Hirschfeld J. Dynamic interactions of neutrophils and biofilms. J Oral Microbiol. 2014;6:26102.
42. Wiseman GM. The hemolysins of *Staphylococcus aureus*. Bacteriol Rev. 975;39(4):317-44.
43. Schindel C, Zitzer A, Schulte B, Gerhards A, Stanley P, Hughes C, et al. Interaction of *Escherichia coli* hemolysin with biological membranes. A study using cysteine scanning mutagenesis. Eur J Biochem. 2001;268:800-8.
44. Ike Y, Hashimoto H, Clewell DB. High incidence of hemolysin production by *Enterococcus* (*Streptococcus*) *faecalis* strains associated with human parenteral infections. J Clin Microbiol. 1987;25:1524-8.
45. Doran KS, Chang JC, Benoit VM, Eckmann L, Nizet V. Group B streptococcal beta-hemolysin/cytolysin promotes invasion of human lung epithelial cells and the release of interleukin-8. J Infect Dis. 2002;185:196-203.
46. Kadioglu A, Weiser JN, Paton JC, Andrew PW. The role of *Streptococcus pneumoniae* virulence factors in host respiratory colonization and disease. Nat Rev Microbiol. 2008;6:288-301.
47. Calderone RA, Fonzi WA. Virulence factors of *Candida albicans*. Trends Microbiol. 2001;9:327-35.

48. Deorukhkar SC, Saini S, Mathew S. Virulence Factors Contributing to Pathogenicity of *Candida tropicalis* and Its Antifungal Susceptibility Profile. Int J Microbiol. 2014;2014:456878.
49. Hurley BP, McCormick BA. Multiple roles of phospholipase A2 during lung infection and inflammation. Infect Immun. 2008;76:2259-2272.
50. Lu H, Que Y, Wu X, Guan T, Guo H. Metabolomics Deciphered Metabolic Reprogramming Required for Biofilm Formation. Sci Rep. 2019;9:13160.
51. Smith AW, Roche H, Trombe MC, Briles DE, Håkansson A. Characterization of the dihydrolipoamide dehydrogenase from *Streptococcus pneumoniae* and its role in pneumococcal infection. Mol Microbiol. 2002;44:431-48.
52. Datta V, Myskowski SM, Kwinn LA, Chiem DN, Varki N, Kansal RG, et al. Mutational analysis of the group A streptococcal operon encoding streptolysin S and its virulence role in invasive infection. Mol Microbiol. 2005;56:681-95.
53. Craig A, Mai J, Cai S, Jeyaseelan S. Neutrophil recruitment to the lungs during bacterial pneumonia. Infect Immun. 2009;77:568-75.
54. Ghoneim HE, Thomas PG, McCullers JA. Depletion of alveolar macrophages during influenza infection facilitates bacterial superinfections. J Immunol. 2013;191:1250-1259.
55. Liu J, Pang Z, Wang G, Guan X, Fang K, Wang Z, et al. Advanced Role of Neutrophils in Common Respiratory Diseases. J Immunol Res. 2017;6710278
56. Sodhi CP, Nguyen J, Yamaguchi Y, Werts AD, Lu P, Ladd MR, et al. A Dynamic Variation of Pulmonary ACE2 Is Required to Modulate Neutrophilic Inflammation in Response to *Pseudomonas aeruginosa* Lung Infection in Mice. J Immunol. 2019;203:3000-12.

57. Aggarwal S, Ahmad I, Lam A, Carlisle MA, Li C, Wells JM, et al. Heme scavenging reduces pulmonary endoplasmic reticulum stress, fibrosis, and emphysema. JCI Insight. 2018;3:e120694.
58. Raval CM, Lee PJ. Heme oxygenase-1 in lung disease. Curr Drug Targets. 2010;11:1532-40.
59. Su WL, Lin CP, Hang HC, Wu PS, Cheng CF, Chao YC. Desaturation and heme elevation during COVID-19 infection: A potential prognostic factor of heme oxygenase-1. J Microbiol Immunol Infect. 2020;S1684-1182:30246-2.
60. Wagener FADTG, Pickkers P, Peterson SJ, Immenschuh S, Abraham NG. Targeting the Heme-Heme Oxygenase System to Prevent Severe Complications Following COVID-19 Infections. Antioxidants (Basel). 2020;9(6):540.
61. Mumby S, Upton RL, Chen Y, Stanford SJ, Quinlan GJ, Nicholson AG, et al. Lung heme oxygenase-1 is elevated in acute respiratory distress syndrome. Crit Care Med. 2004;32:1130-5.
62. Simoni J, Simoni G, Moeller JF, Tsikouris JP, Wesson DE. Evaluation of angiotensin converting enzyme (ACE)-like activity of acellular hemoglobin. Artif Cells Blood Substit Immobil Biotechnol. 2007;35:191-210.
63. Shaver CM, Upchurch CP, Janz DR, Grove BS, Putz ND, Wickersham NE, et al. Cell-free hemoglobin: a novel mediator of acute lung injury. Am J Physiol Lung Cell Mol Physiol. 2016;310:L532-41.
64. Richard KL, Kelley BR, Johnson JG. Heme Uptake and Utilization by Gram-Negative Bacterial Pathogens. Front Cell Infect Microbiol. 2019;9:81.

65. Dutra FF, Alves LS, Rodrigues D, Fernandez PL, de Oliveira RB, Golenbock DT, et al. Hemolysis-induced lethality involves inflammasome activation by heme. Proc Natl Acad Sci U S A. 2014;111:E4110-8.
66. Zheng D, Liwinski T, Elinav E. Inflammasome activation and regulation: toward a better understanding of complex mechanisms. Cell Discov. 2020; 6:36.
67. de Rivero Vaccari JC, Dietrich WD, Keane RW, de Rivero Vaccari JP. The Inflammasome in Times of COVID-19. Front Immunol. 2020;11:583373.
68. Gupta R, Shah P, Swiatlo E. Differential gene expression in *Streptococcus pneumoniae* in response to various iron sources. Microb Pathog. 2009;47:101-9.
69. Kang D, Kirienko NV. Interdependence between iron acquisition and biofilm formation in *Pseudomonas aeruginosa*. J Microbiol. 2018;56:449-57.
70. Hammer ND, Skaar EP. Molecular mechanisms of *Staphylococcus aureus* iron acquisition. Annu Rev Microbiol. 2011;65:129-147.
71. Skaar EP, Humayun M, Bae T, DeBord KL, Schneewind O. Iron-source preference of *Staphylococcus aureus* infections. Science. 2004;305:1626-8.
72. Ledala N, Zhang B, Seravalli J, Powers R, Somerville GA. Influence of iron and aeration on *Staphylococcus aureus* growth, metabolism, and transcription. J Bacteriol. 2014;196:2178-89.
73. Fourie R, Kuloyo OO, Mochochoko BM, Albertyn J, Pohl CH. Iron at the Centre of *Candida albicans* Interactions. Front Cell Infect Microbiol. 2018;8:185.

Address for correspondence: Ana Tereza Ribeiro de Vasconcelos, Laboratório de Bioinformática, Laboratório Nacional de Computação Científica, Avenida Getúlio Vargas 333, Quitandinha Petrópolis, Rio de Janeiro, 25651-076, Brasil; email: atrv@lncc.br.

Table1. Summary of the clinical and demographic aspects of the 21 COVID-19 patients analyzed.

Samples ID*	CT RT-PCR - N1	CT RT-PCR - N2	Intervals (first symptom sampling) (days)	Age range (years)	Sex	Risk factor	Ventilation use	X-ray	Chest computed tomography	Hospitalization (days)	Death
BH1	22.36	28.23	4	80 -90	Male	Obesity; advanced age	Yes; invasive	Mixed	Not performed	28	Yes
BH2	34.75	26.81	5	80 -90	Female	Advanced age	Yes; invasive	Interstitial infiltrate	Not performed	6	Yes
BH3	26.52	29.57	5	50-60	Male	Immunocompromised	Yes; invasive	Interstitial infiltrate	Not performed	55	No
BH4	26.8	29.3	5	50-60	Female	Diabetes; obesity	Yes; invasive	Interstitial infiltrate	Not performed	23	No
BH5	20.2	19.92	6	40-50	Male	Diabetes; hypertension	Yes; invasive	Interstitial infiltrate	Not performed	7	Yes
BH6	33.59	37.28	6	80 -90	Male	Advanced age	Yes; invasive	Interstitial infiltrate	Not performed	11	Yes
BH7	33.89	37.66	7	40-50	Male	Diabetes; hypertension; ex-smoker	Yes; invasive	Interstitial infiltrate	Not performed	60	Yes
BH8	29.2	30.6	7	30-40	Male	Diabetes	Yes; invasive	Normal	Not performed	3	Yes
BH9	19.7	25.3	7	60-70	Male	Diabetes; obesity; hypertension; advanced age	Yes; invasive	Interstitial infiltrate	Not performed	2	Yes
BH10	17.98	18.97	7	40-50	Female	Obesity	Yes; invasive	Consolidation	Not performed	7	Yes
BH11	18.63	20.73	8	40-50	Female	Diabetes; chronic heart disease	Yes; invasive	Interstitial infiltrate	Not performed	10	Yes
BH12	25.46	26.56	8	50-60	Male	Retocolitis	Yes; not invasive	Mixed	Not performed	17	No
BH13	27.87	29.36	9	60-70	Female	COPD; diabetes; obesity; hypertension	Yes; invasive	Interstitial infiltrate	Not performed	10	Yes
BH14	16.94	18.15	10	50-60	Female	Obesity; chronic heart disease	Yes; invasive	Interstitial infiltrate	Not performed	13	Yes
RJ1	24	26	11	50-60	Male	Obesity; hypertension	Yes; invasive	Not performed	COVID suggestive with WITH 50-75% damage	17	No

BH15	26	29.5	12	60-70	Male	Diabetes; chronic heart disease; advanced age	Yes; invasive	Not performed	Not performed	18	Yes
BH16	35.56	32.73	15	70-80	Male	Diabetes; chronic heart disease; advanced age	Yes; invasive	Not performed	Not performed	2	Yes
BH17	15.9	16.3	16	60-70	Female	Hypertension; advanced age	Yes; invasive	Mixed	Not performed	6	Yes
BH18	24	28	16	80 -90	Female	Chronic heart disease; advanced age	Yes; invasive	Interstitial infiltrate	Not performed	10	No
RJ2	32	32	18	50-60	Male	None	Yes; invasive	Not performed	Ground-glass images and consolidation areas with impairment of about 25-50% of the lung parenchyma	20	No
RJ3	30	32	34	70-80	Female	Diabetes; hypertension; advanced age	Yes; invasive	Not performed	Pulmonary damage >50%	37	Yes

* Sample IDs were modified to preserve the patient's integrity.

Table 2. Abundance of the fifty most prevalent species obtained from COVID-19 patients using MG-RAST inference.

Species	BH1	BH2	BH3	BH4	BH5	BH6	BH7	BH8	BH9	BH10	BH11	BH12	BH13	BH14	RJ1	BH15	BH16	BH17	BH18	RJ2	RJ3
Acinetobacter baumannii	150	78	460	5	31	91	462	100	161	6	65	9	78	1443	23845	10	97	482	19	23949	24061
Streptococcus pneumoniae	425	177	357	978	14121	43	577	11	82	4212	5965	2484	67	2563	0	1925	45	154	6364	0	0
Pseudomonas aeruginosa	93	524	225	8	8	58	237	13750	199	389	24	8	311	54	23	41	285	303	7	44	34
Staphylococcus aureus	498	5520	365	152	81	4643	263	29	281	352	210	278	138	720	0	1653	181	209	142	0	0
Enterococcus faecalis	197	401	233	535	620	174	343	16	137	460	497	1326	78	343	0	589	128	175	778	0	0
Escherichia coli	85	139	161	27	41	31	165	96	232	32	167	55	216	140	74	59	206	192	65	104	102
Listeria monocytogenes	220	79	275	66	72	141	197	6	376	51	124	135	110	124	0	94	246	232	98	0	0

Streptococcus agalactiae	35	17	42	117	140	4	61	3	11	307	120	117	16	63	0	57	10	29	327	0	0
Streptococcus pyogenes	44	26	24	99	137	9	50	5	11	285	116	107	26	63	1	59	4	12	364	0	0
Streptococcus spp.	6	2	12	15	515	1	12	0	1	126	246	41	1	47	0	68	0	5	149	0	0
Acinetobacter spp. ADP1	3	5	32	2	3	2	39	8	20	0	3	1	11	34	350	2	9	40	1	390	394
Bacillus cereus	555	152	890	38	86	349	806	28	1398	72	245	79	374	372	2	107	872	900	72	1	2
Bacillus anthracis	481	136	728	40	72	241	630	35	1228	53	175	66	329	286	0	61	691	673	72	0	0
Bacillus thuringiensis	197	46	304	13	27	130	326	9	549	16	92	32	145	137	0	34	348	333	38	0	0
Burkholderia pseudomallei	59	168	251	4	28	39	228	25	241	16	28	10	351	154	10	50	318	316	4	9	4
Streptococcus suis	56	35	50	121	155	7	69	42	31	370	167	159	32	134	0	96	18	39	368	0	0
Acidovorax spp.	144	877	787	2	9	50	965	18	254	28	25	3	1522	89	1	160	1073	1002	5	0	6
Comamonas testosteroni	8	231	221	0	2	7	292	7	65	11	6	1	493	18	1	46	348	334	2	0	0
Cupriavidus metallidurans	33	140	129	2	4	11	146	23	75	3	16	1	239	32	1	26	193	204	3	2	1
Streptococcus mitis	61	17	50	145	1571	6	56	0	12	358	646	236	4	263	0	194	4	18	717	0	0
Pseudomonas putida	16	2727	64	3	6	15	60	124	24	4	8	6	91	12	3	15	86	80	4	12	10
Stenotrophomonas maltophilia	380	81	78	0	8	84	61	9	630	15	43	17	122	328	4	37	381	77	17	24	1
Delftia acidovorans	35	3895	3129	0	2	13	3868	2	67	101	12	1	6808	23	0	693	4336	4359	2	3	0
Coprobacillus spp.	3061	322	414	113	206	232	158	198	640	3	1335	24	471	829	260	42	297	103	420	2	3
Enterococcus faecium	271	201	167	155	241	119	227	1	196	188	276	322	65	211	0	206	146	151	327	0	0
Staphylococcus epidermidis	129	54	126	42	12	12147	42	2	93	328	23	439	56	200	0	4022	40	50	26	0	0
Bifidobacterium dentium	20	12	456	11	3	1	10	0	0	4	9	457	17	584	0	8	2	26	7	0	0
Clostridium difficile	403	16	109	92	67	16	123	7	74	1802	642	141	77	133	0	151	44	39	126	1	0
Granulicatella adiacens	19	265	8	261	289	1	39	1	2	44	164	396	2	106	0	145	3	10	512	0	0
Streptococcus salivarius	8	1	10	486	111	8	46	0	1	57	137	126	22	40	0	46	0	2	1611	0	0
Streptococcus anginosus	37	1	36	12	12	2	80	0	1	2124	200	15	12	35	0	8	8	0	33	0	0

Rothia mucilaginosa	44	1	134	16	131	1	44	1	0	13	58	46	2	847	0	3963	0	6	662	0	0
Atopobium parvulum	156	30	58	1193	36	1	44	0	5	246	332	768	36	392	0	1009	1	271	45	0	0
Actinomyces odontolyticus	70	4	38	120	39	11	189	0	3	12	140	2744	14	226	0	684	0	58	43	0	0
Streptococcus parasanguinis	57	25	73	334	346	2	103	0	0	282	212	498	1	508	0	180	3	88	1629	0	0
Parvimonas micra	338	10	15	84	4	2	119	0	0	1309	747	36	284	196	0	13	6	1	21	0	0
Streptococcus infantis	16	6	2	14	1315	2	7	1	0	85	388	61	1	72	0	155	1	2	271	0	0
Streptococcus sanguinis	29	12	61	192	242	2	143	1	0	629	210	118	8	108	0	79	4	18	384	0	0
Streptococcus gordonii	47	17	72	94	241	3	103	0	2	684	219	124	10	159	0	66	3	15	359	0	0
Leptotrichia buccalis	36	2	19	9	8	8	6	4	0	15	7	1202	9	6	0	64	0	1	607	0	0
Veillonella parvula	39	1	10	222	36	22	39	2	4	18	62	321	64	63	0	338	1	12	69	0	0
Propionibacterium acnes	232	26	51	14	246	189	71	2	108	13	47	199	92	206	2	104	38	133	13	0	0
Bacillus subtilis	730	179	963	52	77	393	872	28	1361	53	221	61	378	480	5	77	995	1103	75	0	1
Streptococcus thermophilus	24	15	39	704	137	6	91	2	6	150	216	223	35	106	0	66	3	12	2129	0	0
Bifidobacterium longum	26	37	143	68	11	7	22	0	3	17	27	181	944	196	0	127	3	513	68	0	0
Lactobacillus gasseri	21	10	3	1615	3	5	5	0	11	107	6	32	4	2	0	7	6	2	14	0	0
Bacillus coagulans	179	42	181	1	15	86	152	0	329	2	42	4	71	115	1	14	246	185	5	0	0
Acidovorax ebreus	46	130	142	1	5	18	146	8	84	4	12	1	232	22	0	28	160	186	3	2	1
Candida albicans	29580	1104202	1136	21439	53	1407860	0	14	1	248985	8	43	18	72	30	66628	6	1176	3	203	179701
Candida tropicalis	307	803954	6950	189	3	12343	3	2	0	2194	1	19	3	0	1	556	4	2786	0	6	1526

Table 3. Functional pathway of Central Carbohydrate Metabolism, related to virulence factors reported for the species identified in this work.

Level 1	Level 2	Level 3	Frequency
Carbohydrates	Central carbohydrate metabolism	TCA_Cycle	18.0406
Carbohydrates	Central carbohydrate metabolism	Pentose_phosphate_pathway	13.0674
Carbohydrates	Central carbohydrate metabolism	Pyruvate_metabolism_I:_anaplerotic_reactions,_PEP	12.7037
Carbohydrates	Central carbohydrate metabolism	Pyruvate_metabolism_II:_acetyl-CoA,_acetogenesis_from_pyruvate	10.5659
Carbohydrates	Central carbohydrate metabolism	Dehydrogenase_complexes	8.8438
Carbohydrates	Central carbohydrate metabolism	Glycolysis_and_Gluconeogenesis,_including_Archaeal_enzymes	7.6641
Carbohydrates	Central carbohydrate metabolism	Glycolysis_and_Gluconeogenesis	7.2847
Carbohydrates	Central carbohydrate metabolism	Pyruvate_Alanine_Serine_Interconversions	6.9584
Carbohydrates	Central carbohydrate metabolism	Entner-Doudoroff_Pathway	4.7727
Carbohydrates	Central carbohydrate metabolism	HPr_kinase_and_hprK_operon_in_Gram-positive_organisms	2.7760
Carbohydrates	Central carbohydrate metabolism	Glycolate,_glyoxylate_interconversions	1.8322
Carbohydrates	Central carbohydrate metabolism	Pyruvate:ferredoxin_oxidoreductase	1.6865
Carbohydrates	Central carbohydrate metabolism	Glyoxylate_bypass	1.3451
Carbohydrates	Central carbohydrate metabolism	Peripheral_Glucose_Catabolism_Pathways	1.2182
Carbohydrates	Central carbohydrate metabolism	Dihydroxyacetone_kinases	0.8161
Carbohydrates	Central carbohydrate metabolism	Methylglyoxal_Metabolism	0.4227
Carbohydrates	Central carbohydrate metabolism	Ethylmalonyl-CoA_pathway_of_C2_assimilation	0.0018

Table 4. Functional profile of TCA_Cycle pathway, related to virulence factors reported for the species identified in this work.

Level 1	Level 2	Level 3	Function	Total abundance	BH1	BH2	BH3	BH4	BH5	BH6	BH7	BH8	BH9	BH10	BH11	BH12	BH13	BH14	BH15	BH16	BH17	BH18	RJ1	RJ2	RJ3
Carbohydrates	Central carbohydrate metabolism	TCA_ Cycle	Dihydrolipoamide dehydrogenase (EC 1.8.1.4)	34640	5	820	250	485	275	305	14155	175	870	0	35	3390	50	30	2320	80	280	200	65	6120	4730
Carbohydrates	Central carbohydrate metabolism	TCA_ Cycle	Succinate dehydrogenase flavoprotein subunit (EC 1.3.99.1)	19476	18	582	492	144	60	153	1863	231	552	36	6	1560	102	30	1554	177	480	12	81	6591	4752

Carbohydrates	Central carbohydrate metabolism	TCA_Cycle	Isocitrate dehydrogenase [NADP] (EC 1.1.1.42)	18878	8	654	306	62	16	242	2112	156	228	44	10	184	108	22	338	196	360	28	88	7842	5874
Carbohydrates	Central carbohydrate metabolism	TCA_Cycle	2-oxoglutarate dehydrogenase E1 component (EC 1.2.4.2)	15954	12	586	332	40	22	192	1342	220	198	26	16	1102	86	24	1246	172	366	28	82	5582	4280
Carbohydrates	Central carbohydrate metabolism	TCA_Cycle	Citrate synthase (si) (EC 2.3.3.1)	13758	6	516	309	108	18	210	3129	177	225	36	12	933	129	12	405	183	366	63	51	3972	2898
Carbohydrates	Central carbohydrate metabolism	TCA_Cycle	Succinate dehydrogenase iron-sulfur protein (EC 1.3.99.1)	13410	5	285	305	110	25	165	1360	110	370	40	25	1145	50	15	1200	125	370	5	60	4405	3235
Carbohydrates	Central carbohydrate metabolism	TCA_Cycle	Fumarate hydratase class II (EC 4.2.1.2)	6109	13	204	122	49	5	103	1920	66	162	10	9	194	47	8	434	32	159	5	10	1401	1156
Carbohydrates	Central carbohydrate metabolism	TCA_Cycle	Malate:quinone oxidoreductase (EC 1.1.99.16)	4162	0	74	26	5	0	36	676	10	109	0	0	66	5	0	473	16	23	0	21	1509	1113
Carbohydrates	Central carbohydrate metabolism	TCA_Cycle	Dihydrolipoamide dehydrogenase of pyruvate dehydrogenase complex (EC 1.8.1.4)	2532	0	98	218	28	18	40	770	132	18	40	10	264	60	6	430	138	244	8	0	10	0
Carbohydrates	Central carbohydrate metabolism	TCA_Cycle	Isocitrate dehydrogenase [NAD] (EC 1.1.1.41)	686	5	24	0	0	0	12	418	6	0	0	0	182	0	0	20	5	0	6	0	8	0
Carbohydrates	Central carbohydrate metabolism	TCA_Cycle	Isocitrate dehydrogenase [NAD] subunit I, mitochondrial precursor (EC	227	0	112	0	0	0	90	12	0	0	0	0	0	0	0	0	0	0	0	0	0	13

			1.1.1.41)																						
Carbohydrates	Central carbohydrate metabolism	TCA_ Cycle	Isocitrate dehydrogenase [NAD] subunit II, mitochondrial precursor (EC 1.1.1.41)	61	0	26	0	0	0	22	8	0	0	0	0	0	0	0	0	0	0	0	0	0	5
Carbohydrates	Central carbohydrate metabolism	TCA_ Cycle	Succinyl-CoA ligase [GDP-forming] alpha chain (EC 6.2.1.4)	42	0	24	0	0	0	18	0	0	0	0	0	0	0	0	0	0	0	0	0	0	0
Carbohydrates	Central carbohydrate metabolism	TCA_ Cycle	Succinyl-CoA ligase [GDP-forming] beta chain (EC 6.2.1.4)	37	0	21	0	0	0	16	0	0	0	0	0	0	0	0	0	0	0	0	0	0	0
Carbohydrates	Central carbohydrate metabolism	TCA_ Cycle	Citrate lyase gamma chain, acyl carrier protein (EC 4.1.3.6)	28	0	0	0	0	0	0	12	0	0	0	0	11	0	0	5	0	0	0	0	0	0

Table 5. Functional profile of Virulence, Disease and Defense pathway, related to virulence factors reported for the species identified in this work.

Level 1	Level 2	Function	Total abundance	BH1	BH2	BH3	BH4	BH5	BH6	BH7	BH8	BH9	BH10	BH11	BH12	BH13	BH14	BH15	BH16	BH17	BH18	RJ1	RJ2	RJ3
Virulence, Disease and Defense	Adhesion	Fibronectin/ fibrinogen-binding protein	4072	0	10	42	70	28	11	3163	27	0	7	0	402	5	8	203	9	47	40	0	0	0
Virulence, Disease and Defense	Adhesion	Fibronectin binding protein FnbB	106	0	9	0	49	0	0	48	0	0	0	0	0	0	0	0	0	0	0	0	0	0
Virulence, Disease and	Adhesion	Fibronectin binding protein	7	0	7	0	0	0	0	0	0	0	0	0	0	0	0	0	0	0	0	0	0	0

Defense		FnbA																						
Virulence, Disease and Defense	Bacteriocins, ribosomally synthesized antibacterial peptides	Bacitracin export permease protein BceB	517	0	8	0	0	0	21	232	0	0	0	0	32	0	0	224	0	0	0	0	0	0
Virulence, Disease and Defense	Bacteriocins, ribosomally synthesized antibacterial peptides	Bacterocin transport accessory protein	513	0	0	0	0	0	0	475	0	0	0	0	26	0	0	5	0	0	7	0	0	0
Virulence, Disease and Defense	Bacteriocins, ribosomally synthesized antibacterial peptides	Bacteriocin	504	0	0	0	11	6	0	455	0	0	0	0	27	0	0	5	0	0	0	0	0	0
Virulence, Disease and Defense	Invasion and intracellular resistance	Sortase	4120	0	30	56	76	56	0	3094	26	34	0	14	468	18	0	168	6	34	26	0	0	14
Virulence, Disease and Defense	Toxins and superantigens	Export ABC transporter ATP-binding protein	568	0	0	0	18	46	0	283	6	18	0	0	143	0	0	48	0	0	6	0	0	0
Virulence, Disease and Defense	Toxins and superantigens	Streptolysin S export transmembrane permease (SagI)	53	0	0	0	0	0	0	48	5	0	0	0	0	0	0	0	0	0	0	0	0	0
Virulence, Disease and Defense	Toxins and superantigens	Streptolysin S biosynthesis protein D (SagD)	51	0	0	0	0	0	0	51	0	0	0	0	0	0	0	0	0	0	0	0	0	0
Virulence, Disease and Defense	Toxins and superantigens	Streptolysin S export transmembrane permease (SagH)	51	0	0	0	0	0	0	45	6	0	0	0	0	0	0	0	0	0	0	0	0	0
Virulence, Disease and Defense	Toxins and superantigens	CylB multidrug/hemolysin transport	49	0	0	0	0	0	0	0	0	0	0	0	37	0	0	12	0	0	0	0	0	0

		system permease protein																						
Virulence, Disease and Defense	Toxins and superantigens	Streptolysin S biosynthesis protein B (SagB)	31	0	0	0	0	0	0	31	0	0	0	0	0	0	0	0	0	0	0	0	0	0
Virulence, Disease and Defense	Toxins and superantigens	Streptolysin S biosynthesis protein C (SagC)	26	0	0	0	0	0	0	26	0	0	0	0	0	0	0	0	0	0	0	0	0	0
Virulence, Disease and Defense	Toxins and superantigens	Streptolysin S self-immunity protein (SagE)	8	0	0	0	0	0	0	8	0	0	0	0	0	0	0	0	0	0	0	0	0	0

Table 6. Functional profile of Membrane Transport pathway, related to virulence factors reported for the species identified in this work.

Level1	Level2	Function	Total abundance	BH1	BH2	BH3	BH4	BH5	BH6	BH7	BH8	BH9	BH10	BH11	BH12	BH13	BH14	BH15	BH16	BH17	BH18	RJ1	RJ2	RJ3
Membrane Transport	Protein secretion system, Type V	Putative large exoprotein involved in heme utilization or adhesion of ShlA/HecA/FhaA family	4736	0	0	0	8	0	0	422	0	503	0	0	217	0	0	20	0	0	0	0	2039	1527
Membrane Transport	Protein secretion system, Type V	Channel-forming transporter/cytolysins activator of TpsB family	2485	0	8	0	5	0	0	66	0	65	0	0	75	0	0	7	0	0	0	0	1283	976
Membrane Transport	Protein secretion system, Type V	Fimbrial adhesin	1842	0	25	27	0	0	0	27	23	0	0	0	0	16	0	30	18	40	0	13	899	724
Membrane Transport	Protein secretion system, Type VI	IcmF-related protein	1244	0	41	93	0	0	0	267	43	254	0	0	0	73	0	79	47	118	0	0	132	97
Membrane Transport	Protein secretion system, Type VI	Sigma-54 dependent transcriptional regulator	1096	0	132	54	0	0	0	320	54	324	0	0	0	22	0	54	14	78	0	0	20	24
Membrane	Protein	T1SS secreted agglutinin	988	0	5	0	0	0	0	6	5	0	0	0	0	0	0	0	0	6	0	0	502	464

Transport	secretion system, Type I	(RTX)																						
Membrane Transport	Protein secretion system, Type I	Hemophore HasA	230	0	0	0	0	0	0	88	0	142	0	0	0	0	0	0	0	0	0	0	0	0
Membrane Transport	Protein secretion system, Type V	bifunctional outer membrane translocase / extracellular lipase, PlpD	204	0	6	0	0	0	0	31	0	45	0	0	20	0	0	5	0	0	0	0	60	37
Membrane Transport	Protein secretion system, Type VI	Protein phosphatase ImpM	192	0	16	14	0	0	0	54	12	32	0	0	0	10	0	16	16	22	0	0	0	0
Membrane Transport	Protein secretion system, Type VI	Serine/threonine protein kinase (EC 2.7.11.1) PpkA	122	0	0	0	0	0	0	51	0	71	0	0	0	0	0	0	0	0	0	0	0	0
Membrane Transport	Protein secretion system, Type I	Hemophore HasA outer membrane receptor HasR	92	0	0	0	0	0	0	34	0	58	0	0	0	0	0	0	0	0	0	0	0	0
Membrane Transport	Protein secretion system, Type I	type I secretion system ATPase, LssB family (LapB)	82	0	0	0	0	0	0	82	0	0	0	0	0	0	0	0	0	0	0	0	0	0
Membrane Transport	Protein secretion system, Type I	ABC-type protease exporter, ATP-binding component PrtD/AprD	69	0	0	0	0	0	0	26	0	43	0	0	0	0	0	0	0	0	0	0	0	0
Membrane Transport	Protein secretion system, Type I	Secreted alkaline metalloproteinase (EC 3.4.24.-), PrtA/B/C/G homolog	60	0	0	0	0	0	0	31	0	29	0	0	0	0	0	0	0	0	0	0	0	0
Membrane Transport	Protein secretion system, Type I	ABC exporter for hemopore HasA, ATP-binding component HasD	58	0	0	0	0	0	0	25	0	33	0	0	0	0	0	0	0	0	0	0	0	0
Membrane	Protein	Putative	44	0	34	0	0	0	0	0	0	0	0	0	10	0	0	0	0	0	0	0	0	0

Transport	secretion system, Type V	haemolysin/cytolysin secreted via TPS pathway																						
Membrane Transport	Protein secretion system, Type I	ABC exporter for hemopore HasA, membrane fusion protein (MFP) family component HasE	44	0	0	0	0	0	0	21	0	23	0	0	0	0	0	0	0	0	0	0	0	0
Membrane Transport	Protein secretion system, Type I	ABC-type protease exporter, outer membrane component PrtF/AprF	42	0	0	0	0	0	0	15	0	27	0	0	0	0	0	0	0	0	0	0	0	0
Membrane Transport	Protein secretion system, Type I	ABC exporter for hemopore HasA, outer membrane component HasF	37	0	0	0	0	0	0	17	0	20	0	0	0	0	0	0	0	0	0	0	0	0
Membrane Transport	Protein secretion system, Type VI	Secreted protein Hcp	33	0	0	0	0	0	0	15	0	18	0	0	0	0	0	0	0	0	0	0	0	0
Membrane Transport	Protein secretion system, Type VI	Type VI secretion lipoprotein/VasD	33	0	0	0	0	0	0	9	0	24	0	0	0	0	0	0	0	0	0	0	0	0
Membrane Transport	Protein secretion system, Type VI	Inner membrane protein DotU	23	0	0	0	0	0	0	6	0	17	0	0	0	0	0	0	0	0	0	0	0	0
Membrane Transport	Protein secretion system, Type VI	Phosphoprotein phosphatase PppA	23	0	0	0	0	0	0	10	0	13	0	0	0	0	0	0	0	0	0	0	0	0
Membrane Transport	Protein secretion system, Type I	Alkaline proteinase inhibitor precursor	16	0	0	0	0	0	0	10	0	6	0	0	0	0	0	0	0	0	0	0	0	0

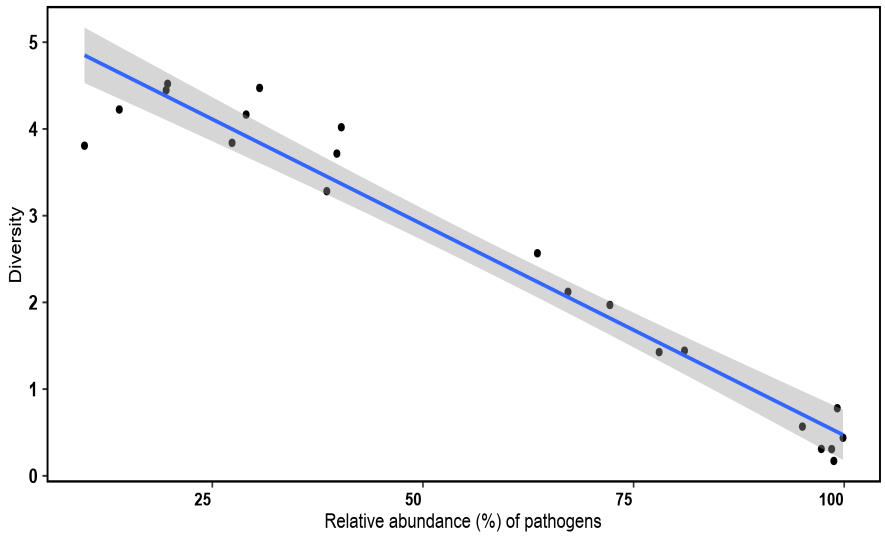

Figure 1. Pearson correlation between the Shannon diversity index and the relative abundance of pathogenic species identified in the 21 COVID-19 patients.

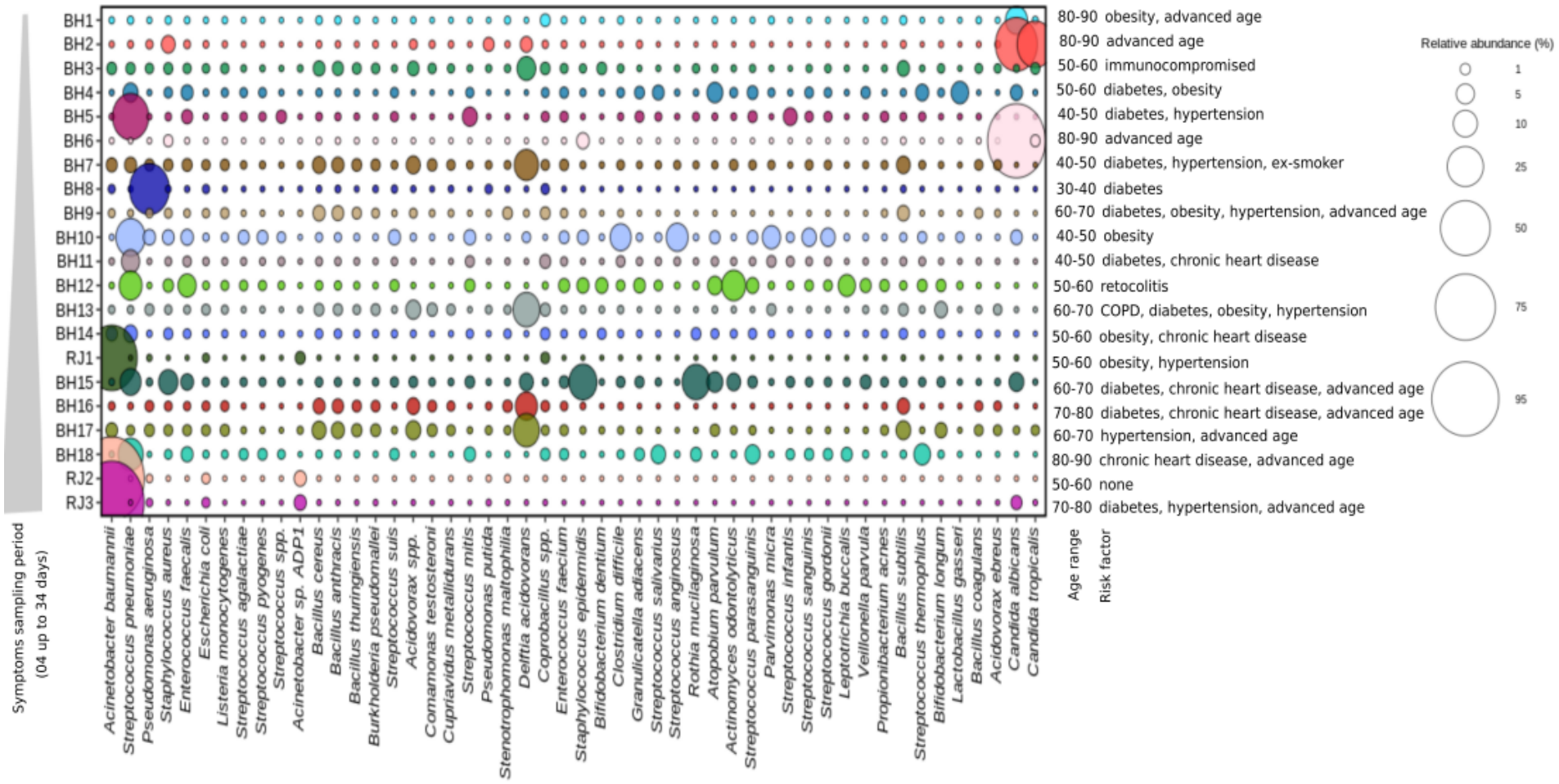

Figure 2. Relative abundance of the 50 most prevalent species identified in the 21 COVID-19 patients. The characteristics of the individuals analyzed, such as age range, comorbidities and time (days) from onset of symptoms until sample collection were represented.

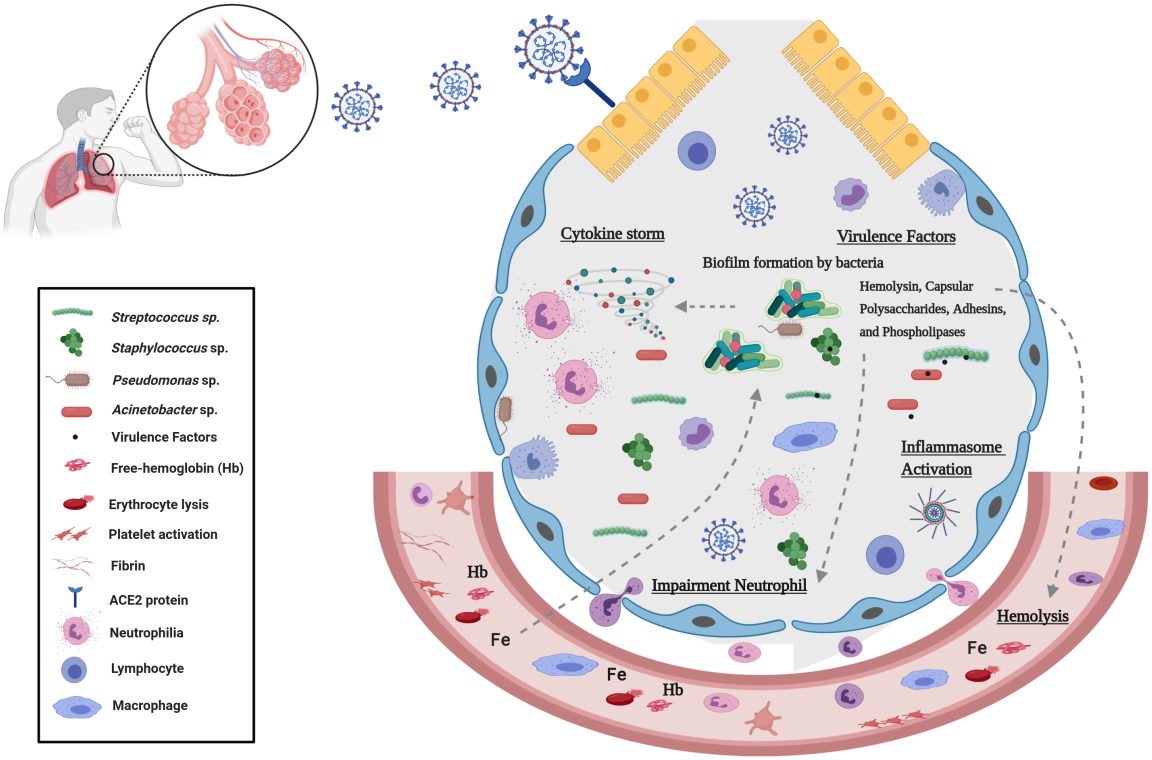

Figure 3. Model for an interplay of the bacteria found in COVID-19 patients, virulence factors and free-iron in immune response and disease severity. In severe lung diseases, hyperventilation contributes to microbial influx and reduces the elimination of microorganisms. Tecidual injury promotes a rich environment for growth of specific lung pathogens into the alveolar compartment. Bacterial pathogens evade the host immune response by biofilm production, induction of hemolysins, iron acquisition factors, adhesins, and other virulence factors. The SARS-CoV-2 and bacterial pathogens promote erythrocyte lysis, causing heme(Hb)/iron(Fe) liberation. Heme uptake is required for bacterial host colonization and increased production of virulence factors. Bacterial virulence factors, as well as free-heme, activates the inflammasome, contributing to neutrophil inflammation, cytokine elevation and pathogenesis processes. This figure was generated using the BioRender (available at https://biorender.com/).